NANO LETTERS

pubs.acs.org/NanoLett

Bulklike Hot Carrier Dynamics in Lead Sulfide Quantum Dots

Byungmoon Cho, William K. Peters, Robert J. Hill, Trevor L. Courtney, and David M. Jonas*

Department of Chemistry and Biochemistry, University of Colorado, Boulder, Colorado 80309-0215

ABSTRACT Hot electronic dynamics in lead sulfide nanocrystals is interrogated by degenerate pump−probe spectroscopy with 20−25 fs pulses over a broad frequency range around three times the nanocrystal band gap. For each nanocrystal diameter, an initial reduction in absorption is seen only at the peak of the quantum confined E1 transition, while increased absorption is seen at all other wavelengths. The signals from the nanocrystals are ∼300 times weaker than expected for a two-level system with the same absorbance and molar extinction coefficient and are weaker near time zero. These results appear to be inconsistent with quantum confinement of the initially excited high energy states. Arguments based on carrier scattering length, the wave packet size supported by the band structure, and effective mass are advanced to support the hypothesis that, for many direct-gap semiconductor quantum dots, the carrier dynamics at three times the band gap is localized on the 1−2 nm length scale and essentially bulklike except for frequent collisions with the surface.

KEYWORDS Quantum Dots, Carrier Relaxation, Scattering Length, Impact Ionization

The nature and behavior of high energy electronic excitations in semiconductor nanocrystals are important for understanding carrier multiplication, which has possible applications in high efficiency solar cells,[1,2] photodetectors,[3] photocatalysts, and optical amplifiers.[4] Direct photoexcitation,[5] coherent multiple exciton generation,[6] and incoherent impact ionization[7] have been proposed to explain the reported production of multiple electron−hole pairs from a single photon in nanocrystals.[8,9] In bulk semiconductors, a Rydberg series of bound electron−hole pair states (Wannier excitons) starts below the band gap.[10] These states have energies and eigenfunctions like a one electron atom with a Bohr exciton radius $a_0 = 4\pi\varepsilon\hbar^2/\mu e^2$, where ε is the dielectric constant, μ is the reduced mass calculated from the effective masses of the electron and hole, and e is the electron charge. Above the band gap, electrons and holes are excited to states analogous to the atomic ionization continuum and separate as free carriers. High-energy photons can excite nonequilibrium carriers with group velocities exceeding the saturation velocity (∼10^5 m/s in bulk semiconductors[11]). Near the saturation velocity, the rate of energy loss greatly exceeds the Ohm's law scattering rate (which is usually dominated by acoustic phonons).[12]

Following the treatment by Éfros and Éfros,[13] semiconductor nanocrystals with bulk crystalline lattices but diameters smaller than the Bohr exciton radius have been called quantum dots because their absorption and emission spectra near the band gap display quantum confinement blue-shifts with decreasing size. This confinement forces electrons and holes closer together, increasing the Coulomb interaction involved in Auger recombination and its inverse, impact ionization.[14] For strong quantum confinement, the oscillator strength per dot at the band gap is predicted to be independent of size.[15] Although the growth of band gap absorption relative to the higher energy spectrum has abundant experimental support,[16] a size-independent oscillator strength is not always observed.[17]

Because the dense manifold of hot quantum-confined states is predicted to replicate the bulk absorption spectrum,[13] it has been conventionally thought[18] that highly excited states of quantum dots also have a quantum confined character (see chapter 18 of ref 19). However, in an early paper,[20] Brus made a brief suggestion that a rigorous distinction between quantum dots and small pieces of bulk semiconductor might be made on the basis of carrier scattering length. Because the high energy spectrum can be accounted for with either quantum confined or bulklike states, it is important to experimentally characterize the states in this energy range. According to theory,[21,22] quantum confined systems absorb light as a single unit, so that their absorption readily saturates to yield pump−probe signals scaling as εA, where ε is the molar decadic extinction coefficient and A is the absorbance. Indeed, near the band gap, quantum dots have been used as long-lived saturable absorbers.[23] In contrast, the weak field saturated absorption of bulk semiconductors is proportional to $\chi^{(3)}$l, where $\chi^{(3)}$ is the nonlinear susceptibility and l is the sample length.[24] That $\chi^{(3)}$ does not depend on the number of unit cells (N) in the bulk crystal can be understood in two equivalent ways: (1) the absorbing unit is smaller than the crystal so that ε is smaller for each absorbing unit but the number of absorbing units increases so that A remains constant; (2) when the crystal is excited, the saturated absorption (positive signal proportional to N^2) is mostly canceled by systematic excited

* To whom correspondence should be addressed. E-mail: david.jonas@colorado.edu. Tel. (303)492-3818. Fax (303)492-5894.

Received for review: 03/24/2010
Published on Web: 06/15/2010

© 2010 American Chemical Society

DOI: 10.1021/nl1010349 | *Nano Lett.* **2010,** *10,* 2498–2505

state absorption [negative signal proportional to $N(N-1)$].[25] When ε is proportional to N, εA is proportional to N^2, so the resulting pump−probe signal at zero delay is roughly $(1/N)$ weaker in a bulklike system than in a quantum confined system. In molecular aggregates, this reduction in the size of the absorbing unit arises from disorder and coupling to phonons, both of which cause carrier scattering in bulk semiconductors. Excitation by a coherent pulse will prepare a coherent superposition of excited states that both maximizes stimulated emission and minimizes absorption for an identical probe,[26] these positive contributions to the signal scale as εA. The dephasing and lifetime decay that reduce the signal from this coherent superposition of excited electronic states can occur through both production of multiexciton states and competing carrier scattering; carrier scattering has been estimated to take place on time scales ranging from 50 fs (ref 5) to 3 ps (ref 27) with most estimates ranging from 100 fs to 1 ps.[7,28,29]

In this letter, we report experiments that suggest quantum dots act as small pieces of bulk semiconductor for hot carriers. Importantly, we show these results on the relaxation of hot carriers over the first 2 ps are insensitive to the apparent multiexciton yield, multiphoton excitation, and other difficulties[30−36] involved in studying multiple exciton generation. Therefore, this letter concentrates on robust conclusions about relaxation during the first 2 ps after photoexcitation. We then discuss the scattering length using the bulk band structure; this discussion shows that quantum-confined states (with properties different from the photoexcited states in the bulk) should not be expected for the high energy excitations that produce hot carriers in the bulk.

Bulk PbS has a rock salt structure, a small direct band gap (0.42 eV at 300 K), small electron and hole effective masses ($m_e^* = m_h^* = 0.105m_e$, where m_e is the rest electron mass), and a large high frequency dielectric constant ($\varepsilon_\infty = 17$).[37] With $a_0 \geq 17$ nm, PbS nanocrystals show strong quantum confinement.[38] Reported multiexciton yields vary significantly between experiments,[6,31,35] possibly due to differences between probe methods, sample synthesis and handling,[31] pulse fluence,[30] or sample refreshing.[34,39] We measure degenerate pump−probe signals for nanocrystals relative to the signals for "slow" saturable absorber dyes,[40] which act as electronic two-level systems with known signal strengths scaling as εA. The measurements employ low fluence pulses of 20−25 fs duration and a rapidly spinning, vacuum-tight sample cell to completely refresh the sample after every laser shot.

PbS nanocrystals capped with oleate ligands and dispersed in toluene were purchased from Evident Technologies because production of multiexciton states has been reported in samples synthesized by Evident.[6] The first batch of 8 nm diameter nanocrystals was custom synthesized, shipped in a colored glass bottle without an airtight seal, kept in a refrigerator, and put into airtight sample cells under open air for measurements completed within 10 weeks of the order; it showed signatures conventionally attributed to production of multiexciton states (see below). A second batch of 8 nm nanocrystals, synthesized the same week as the first, was purchased 9 months later and split into two sets: one was handled as above; the other was freeze-pump thawed to remove oxygen, kept in a nitrogen-purged glovebox, and put into airtight sample cells inside the glovebox. The 5 and 4 nm diameter PbS nanocrystal samples were purchased as stock sizes and also divided into two sets. These smaller nanocrystals and the second 8 nm batch showed greatly reduced, if any, signatures of production of multiexciton states.

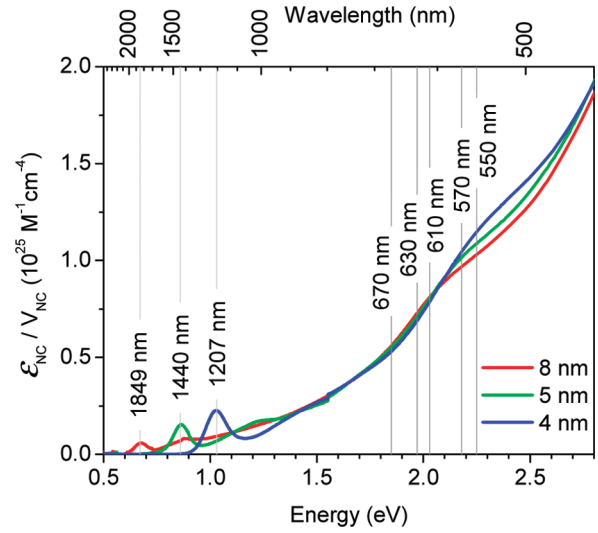

FIGURE 1. Volume normalized molar decadic extinction coefficients of oleate capped PbS nanocrystals in toluene for three nanocrystal diameters: 8 nm (red curve), 5 nm (green curve), and 4 nm (blue curve).

The molar decadic extinction coefficient per PbS nanocrystal volume is shown for 8, 5, and 4 nm diameters in Figure 1. The quantum confined first exciton peaks at 0.68, 0.86, and 1.03 eV, respectively, derive from the bulk band gap at the L point of the first Brillouin zone.[19] It is known that the absorption cross section becomes proportional to the nanocrystal volume at high photon energy,[13,17,41,42] and this is noticeable for the rising absorption background in Figure 1. The weak shoulders at 2.14, 2.21, and 2.30 eV, respectively, on top of the rising background derive from the E1 transition of bulk PbS (assigned as either a valence to conduction band transition at the Σ_5 point[43] or as the same transition overlapping with a valence to second conduction band transition at the L point[44]). By analogy to PbSe,[45] these shoulders represent the first exciton peak of the PbS E1 transition. Compared to the bandgap, they show a smaller quantum confinement blue shift with decreasing nanocrystal size,[41] which should be expected from the larger effective masses (hence smaller Bohr exciton radii).[45,46]

The femtosecond pump/probe pulses were generated from a home-built noncollinear optical parametric amplifier (NOPA),[47] pumped by a 50 fs, 800 nm, 6 μJ regenerative

© 2010 American Chemical Society

DOI: 10.1021/nl1010349 | *Nano Lett.* **2010,** *10,* 2498--2505

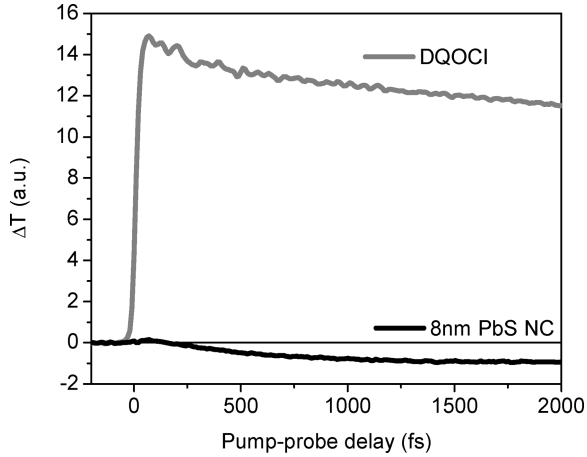

FIGURE 2. Pump−probe signal ΔT for 8 nm diameter PbS nanocrystals (black) compared to ΔT for the saturable absorber DQOCI (gray) under the same conditions: 610 nm excitation/probe wavelength; 10 nJ pump and 0.5 nJ probe pulse energies; 25 fs pulse duration; 200 μm beam diameter; 10 kHz laser repetition rate; 1800 rpm sample spin rate; absorbance $A = 0.4$ (PbS); $A = 0.4$ (DQOCI). For DQOCI, Beer's law estimates indicate about 1% of the molecules are excited (implying $\Delta T_{max} \sim +0.004$ at ~15 on the vertical scale).

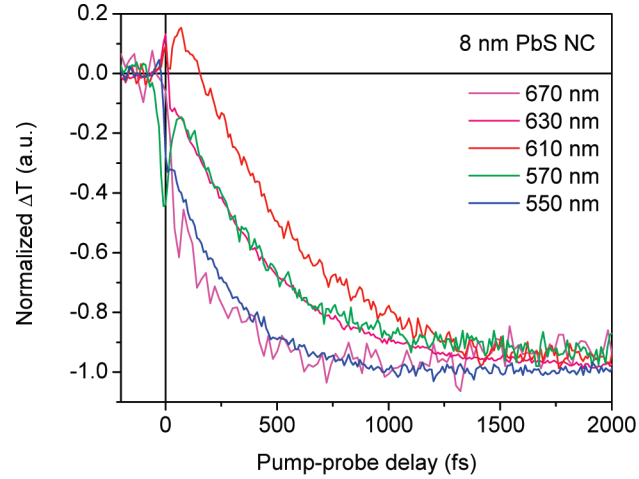

FIGURE 3. The degenerate pump−probe signal for 8 nm diameter PbS nanocrystals as a function of pump−probe wavelength. Experimental parameters are the same as Figure 2. The signals are normalized at 2 ps to highlight differences in the fast relaxation, which are dominated by excitation of the E1 transition centered at 610 nm.

amplifier running at 10 kHz repetition rate (Coherent RegA 9060). NOPA output of up to 150 nJ was generated with bandwidths ranging from 25−40 nm in the 500−700 nm wavelength range. The NOPA pulses were compressed with a pair of fused-silica prisms and were characterized by second harmonic generation frequency resolved optical gating[48] in a 100 μm thick Type I KDP crystal. The pulse durations recovered were ~20−25 fs. A dielectric beamsplitter divided the NOPA pulses into pump and probe pulses. The probe passed through a compensating block of the same material as the beamsplitter before a variable delay set by a computer-controlled translation stage. The pump and probe propagated on parallel paths into a reflective Cassegrain telescope, after which they crossed in the sample with a 200 μm diameter (as measured by 50% transmission through a pinhole). Pump excitation probabilities were varied from 1 to 40% (0.5−20 nJ for 8 nm diameter PbS at 610 nm wavelength). The probe energy was fixed at 0.5 nJ. The pump was chopped at 500 Hz and the pump−probe signal, defined as the pump-induced increase in probe transmission, ΔT, was measured with a Si photodiode and lock-in detector referenced to the pump chopping frequency. The vacuum-tight sample cell was spun at ~1800 rpm and probed about 1 cm off-axis, ensuring a fresh sample for each laser shot, but probing the same volume again after a 33 ms delay. This is much longer than the ~4 μs excited state lifetime,[49] but (unfortunately) shorter than the dark state off times observed in single dot spectroscopy.[50]

The pump−probe signal from 8 nm diameter PbS nanocrystals is shown in Figure 2 as the negative-going black line (negative signals indicate the pump reduces probe transmission). On the same graph, the pump−probe signal, measured with identical pulses (25 fs duration at 610 nm), for a solution of the saturable absorber dye DQOCI (an electronic two-level system) with the same absorbance ($A = -\log_{10}(T) = 0.4$) is shown as the positive-going gray line. Since the first excited electronic state of a saturable absorber does not absorb light at wavelengths within the first electronic absorption band, the absorbance change upon excitation of a fraction of molecules f is $\Delta A \sim -fA$ (f is proportional to ε). Although the 8 nm nanocrystal's molar extinction coefficient is 20× larger than that of DQOCI, so that ΔT should be 20× larger for the nanocrystals, the initial pump−probe signal from the PbS nanocrystals is nearly zero. At one wavelength, signal could vanish through accidental cancellation of positive (excited state emission plus reduced ground state absorption) and negative (excited state absorption) contributions, but a near zero signal was measured for 7 pump−probe wavelengths between 507 and 670 nm.

A nanocrystal absorbing as one unit is inconsistent with this result; the absorbing unit must be much smaller. When the maximum absorption increase is reached at 2 ps delay, the signal is ~1/15 of that from DQOCI. The small increase in absorption (negative signal) at 2 ps delay is consistent with the excited state having an absorption spectrum that is a red-shifted (by ~1 meV) replica of the ground-state absorption spectrum. Because the steady-state change in the spectrum caused by photoexcitation resembles that caused by a static electric field, it has been attributed to an internal Stark effect caused by charge redistribution in the nanocrystal.[51]

Figure 3 shows the wavelength dependent early time dynamics. An initial positive signal occurs only for 610 nm excitation, which maximally excites the weak shoulder arising from the first exciton peak of the bulk E1 transition.[52] For excitation pulse spectra partially overlapping the E1 transition, E1 excitation adds a short-lived (~100 fs) positive (two-level like) signal of the kind discussed in ref 21 to the

© 2010 American Chemical Society

DOI: 10.1021/nl1010349 | *Nano Lett.* **2010,** *10,* 2498--2505

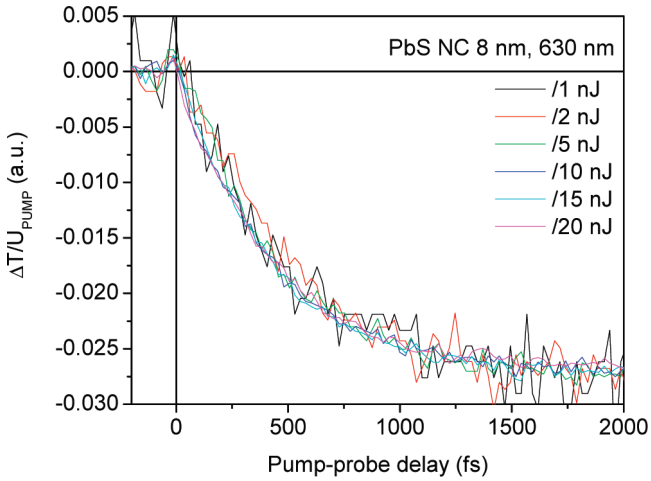

FIGURE 4. The pump−probe signal divided by the pump pulse energy at constant 0.5 nJ probe pulse energy; 630 nm pump and probe wavelength; 25 fs pulse duration; 200 μm beam diameter; 10 kHz laser repetition rate; 1800 rpm sample spin rate; absorbance A = 0.4 at 610 nm. The pump pulse energies were 1 (2%), 2 (4%), 5 (10%), 10 (20%), 15 (30%), and 20 nJ (40%) (numbers in parentheses indicate the corresponding excitation probabilities).

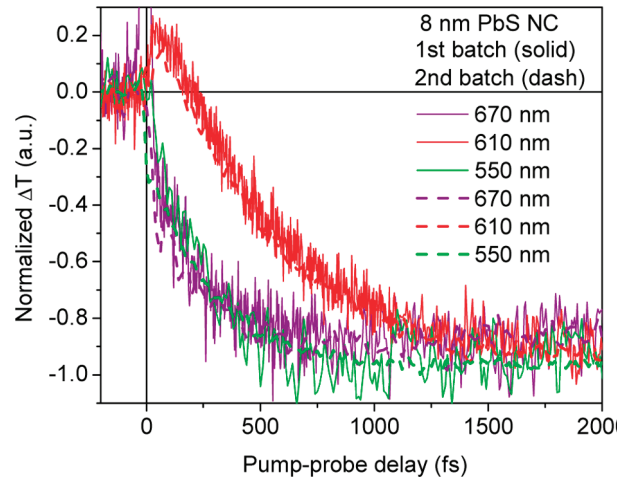

FIGURE 5. Initial dynamics for two batches with different dynamics on 100 ps timescales: The first batch showed long-time decay roughly matching the bi-exciton lifetime, and the second batch did not. Experimental parameters for the first batch are: 2.5 nJ pump and probe pulse energies; 25 fs pulse duration; 100 μm beam diameter; 20 kHz laser repetition rate; 1800 rpm sample spin rate; and absorbance A = 0.6 (at 610 nm). Experimental parameters for the second batch are the same as in Figure 2.

negative excited state absorption signal. Our interpretation is that the signals at 550 and 670 nm essentially represent the dynamics of the hot states excited via the smooth background underneath the E1 shoulder. These hot states show an initial increase in absorption at $T = 0$, which further increases by about a factor of 2 with a 240 fs time constant until the full Stark red shift is developed.[51] Other experiments[6,53] and theory[54] suggest that carrier cooling to the band gap is completed during this time. As the wavelength is tuned toward the peak of the E1 transition, a positive signal from nanocrystals excited via the E1 shoulder is added to the negative signal from nanocrystals excited via the smooth background. Nanocrystals excited to the quantum confined E1 state decay with a ~100 fs lifetime via intervalley scattering into high energy states similar to those excited directly via the smooth background; these hot states then relax with about the same time constant as the directly excited high energy states. Before this relaxation, the magnitude of the signal from direct photoexcitation of the hot states is thus about 600× smaller [(1/2)(1/15)(1/20)] than expected for quantum confinement; except for the sign, this is in reasonable agreement with the bulk prediction (1200× smaller) .

Figure 4 shows the 8 nm diameter PbS nanocrystal pump−probe signals at different excitation pulse energies. When the signals are divided by the respective pump pulse energies, the traces overlap, so the early time dynamics is independent of the excitation probability up to 40% excitation, when the Poisson distribution predicts ~23% of the signal comes from nanocrystals with two or more excitations. Within the precision of the data, the relaxation of one hot electron−hole pair is unaffected by another until at least 2 ps delay (barring filling of the 8-fold degenerate conduction band, which occurs at much higher pulse fluences); the hot carriers thus behave as if uncoupled to one another, as in the bulk.

Figure 5 compares the pump−probe signals from the first 8 nm batch to signals from the second 8 nm batch (handled in the same way, not deoxygenated) at three different excitation wavelengths. For PbSe nanocrystals, photo-oxidation causes a blue shift of the first exciton peak.[55] Approximately 1 meV blue shifts were observed here in PbS nanocrystals after two weeks exposure to dissolved oxygen and the laser beam. Deoxygenation by freeze−pump−thawing inhibited the blue shift, but had no significant effect on the signal (data not shown). However, for higher photon energies, the signal from the first 8 nm diameter batch decayed for delays longer than 2 ps (not shown): the signals measured at 610, 550, and 537 nm decay to half of their 2 ps amplitude with time constants of 100−180 ps, roughly matching the biexciton lifetime of ~120 ps (determined by using the model of ref 56 to fit the pulse energy dependent signals after multiphoton excitation of the first 8 nm batch at 800 nm). The conventional interpretation[8] would be 70−100% yield of the biexciton above three times the nanocrystal band gap; however, yield determination is controversial.[30−32,35,57] For the smaller nanocrystals and the second 8 nm batch, the data are consistent with 0% yield and inconsistent with any yield above 10% (except at 610 nm for the second 8 nm batch, where low signal-to-noise longer scans are compatible with up to 30% yield). This variation in dynamics for 8 nm diameter nanocrystals on 100 ps time scales may be related to nanocrystal synthesis, storage, or handling. Figure 5 shows that the relaxation of hot carriers over the first 2 ps is not sensitive to nanocrystal handling or biexciton signatures.

© 2010 American Chemical Society

DOI: 10.1021/nl1010349 | *Nano Lett.* **2010,** *10,* 2498--2505

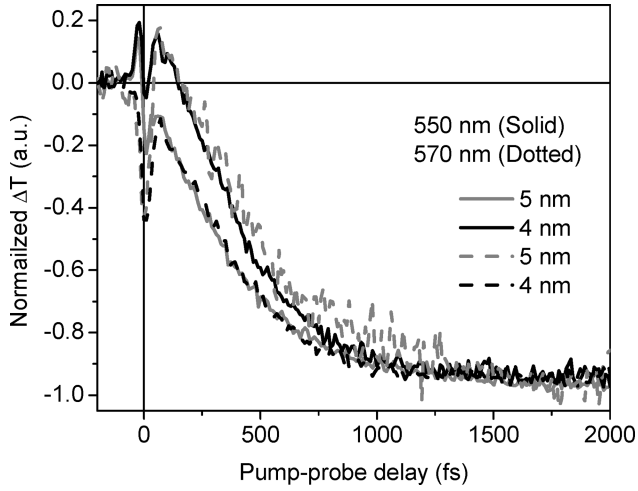

FIGURE 6. Comparison between degenerate pump−probe signals for 4 nm (black) and 5 nm (gray) diameter PbS nanocrystals at 550 nm (solid) and 570 nm (dotted) wavelengths. All signals are normalized at 2 ps pump−probe delay. 550 nm (570 nm) excites the peak of the E1 transition for 4 nm (5 nm) diameter nanocrystals. The pump pulse energy at 550 nm was 20 nJ, yielding excitation probabilities of 17% (5 nm) and 6% (4 nm). The pump pulse energies at 570 nm were 15 nJ (5% excitation probability for 4 nm diameter) and 17 nJ (14% excitation probability for 5 nm diameter). (The weakness of these signals is illustrated by the negative spikes at $T = 0$, which are observed for neat toluene and might arise from probe focusing changes caused by the instantaneous pump-induced change in solvent refractive index.) Sample absorbance at 610 nm: $A = 0.4$ (5 nm) and $A = 0.6$ (4 nm). All signals used 0.5 nJ probe pulse energy, 25 fs pulse duration, 200 μm beam diameter, 10 kHz laser repetition rate, and 1800 rpm sample spin rate.

Figure 6 shows the initial positive signal observed when pumping and probing at the quantum confined E1 transition in the 4 and 5 nm diameter nanocrystals. As for the 8 nm diameter (Figure 3), the degenerate pump−probe signal is small compared to that from saturable absorbers with the same absorbance and negative at all wavelengths measured between 507 and 670 nm other than the E1 maximum. Given the weakness of the E1 shoulder, it is surprising that the positive signal from E1 excitation is strong enough to cancel the negative signal from the larger smooth background. Quantum-confined states produce more signal for a given extinction coefficient than the hot states.

A priori, three conclusions seem possible: (1) Some nanocrystals, including those studied here, have surfaces that do not support hot quantum-confined states; (2) hot states of nanocrystals are quantum confined but systematically different from the lowest quantum-confined state in always having excited state absorption that almost perfectly cancels the reduced absorption and emission contributions; or (3) the hot states are bulklike, not quantum confined, and relax independently of one another for the first 2 ps. Under hypothesis 1 or 3, the absence of positive signal during the pump pulse would require destruction of the coherently excited hot state on a time scale much shorter than the pulse duration, perhaps ∼5 fs. Noting that the convergence of quantum dot absorption spectra to that of the bulk at photon energies around three times the nanocrystal band gap is consistent with all three hypotheses, we now turn to theoretical arguments, based on bulk properties, that support the bulklike hypothesis. Suggestions that the bulk band structure cannot be used because the envelope functions for a nanocrystal are entirely different from Bloch waves and lack translational symmetry are not useful because they prove too much; the same argument applies to any finite bulk solid. Effective masses from the bulk band structure develop at a very short length scale,[20] justifying their use at the core of quantum confinement theory.[13,20] Differences in quantum confinement blue shifts for different features of the bulk spectrum have long been explained as arising from differences in effective mass at different critical points in the band structure.[45,46] The view delineated here is that if the electronic state and its interactions in the bulk can be localized on length scales smaller than the nanocrystal dimensions, then these spatially localized properties and interactions will persist in the nanocrystal.

Such localization criteria can be valid independently of the surface and nonlinear optical properties involved in the first two hypotheses mentioned above. Accordingly, we use the bulk band structure of PbS[44] and the pulse spectrum to estimate carrier wave packet properties. We first find the vertical excitation wave-vector along Λ [the line between the Γ point at $\mathbf{k} = (0,0,0)$ and the L points at $\mathbf{k} = (\pm\pi/a, \pm\pi/a, \pm\pi/a)$[19] where $a = 5.94$ Å is the lattice constant[37]] at which the gap $\Delta E_g = E_c - E_v$ between the conduction and valence bands matches the energy of a 600 nm photon; this occurs at $\mathbf{k} \sim 0.7(\pm1, \pm1, \pm1)(\pi/a)$. The group velocity for an electron is $v_g^e = (1/\hbar)dE_c/dk$,[10] where dE_c/dk is the slope of the conduction band and $\hbar$ is the reduced Planck constant; at the vertical excitation wave-vector, the electron group velocity is 9×10^5 m/s and the hole group velocity $v_g^h = (1/\hbar)dE_v/dk$ is 6×10^5 m/s in the valence band. Near this vertical excitation wave-vector, the curvatures of both the valence band and the conduction band are near vanishing; the effective masses $[m^*_{e,h} = \pm\hbar^2/(\partial^2 E_{c,v}/\partial k^2)]$[10] of the electron and hole have gone up by at least a factor of 10 as they diverge to infinity. Such diverging effective masses are expected at some point above the band gap in all direct gap semiconductors.[10] This divergence sends the Bohr exciton radius to zero, so quantum confinement effects should not be expected at these points in the band structure. This extension of the effective mass theory for quantum confinement effects from critical points to the entire band structure does not yet establish that the envelope functions of the nanocrystal support the dynamics of the bulk band structure.

The relevance of bulklike dynamics to the nanocrystal can be established from the size of the carrier wave-packets supported by the band structure and the length scale of their interaction with phonons. A Gaussian wavepacket with probability full width at half-maximum Δk has a transform-limited spatial probability full width at half-maximum $\Delta r \Delta k = 4\ln(2)$. Around the vertical excitation point along Λ, the

© 2010 American Chemical Society

DOI: 10.1021/nl1010349 | *Nano Lett.* **2010,** *10,* 2498--2505

bulk band structure indicates near constant group velocities (hence near diverging effective masses) from $k \sim$ (0.2 to 0.8)$(3)^{1/2}(\pi/a)$, supporting carrier wave-packets smaller than 2 unit cells in width (~1 nm). From the group velocities, such electron and hole wavepackets will rapidly (~3 fs) separate into free carriers. The length scale for their interaction with the lattice is given by the size of the polaron (lattice distortions around free carriers). From eq 10.23 in ref 10, the polaron radii are about 3.8 nm at the PbS band gap, drop by at least a factor of 3 at the vertical excitation point, and tend toward zero as the effective masses diverge. In the bulk, carrier interactions with the lattice involve scattering lengths and polaron radii much smaller than the size of the nanocrystals in these experiments. These local interactions should be the same when wave-packets with the same properties are built from the complete set of nanocrystal envelope functions; this indicates the strength of these interactions with the lattice must be, in some average sense, similar for plane-wave and nanocrystal envelope functions.

Group velocities from the bulk band structure can be used to assess the time and length scales for carrier scattering processes. Since the group velocities are much greater than the fastest phonon group velocities (based on the dispersion relations in ref 58, these are ~7000 m/s in bulk PbS), the carriers leave optical and acoustic phonon wakes as they propagate. More importantly, these velocities are much greater than the 10^5 m/s saturation velocity that the field-induced drift velocity cannot exceed in bulk semiconductors.[11,59] The Ohm's law scattering length for PbS calculated from the mobility μ in ref[37] using $l = (3\mu/4e)(2\pi m^* k_B T)^{1/2}$ [eq 28b in chapter 11 of ref 60] is 14 nm; l depends on temperature through the phonons that cause scattering, but is independent of electron velocity [see the discussion below eq 30 in chapter 17 of ref 60]. Therefore, the mean scattering time $\tau = l/v$ is inversely proportional to velocity in the Ohm's law regime.[12,60] For hot carriers, new scattering channels become accessible and the inelastic scattering length[61] can be over an order of magnitude shorter than the Ohm's law scattering length.[62] At a velocity of 0.9 nm/fs, electron scattering via impact ionization and optical phonons is thus expected to occur perhaps an order of magnitude more often than the Ohm's law mean scattering time of 16 fs. The above discussion indicates that for hot states in PbS nanocrystals, bulklike electron−phonon inelastic scattering on a time scale of ~5 fs or shorter, as inferred from the experiments, is plausible. The electron and hole also collide frequently with the surface; for an 8 nm diameter nanocrystal, an electron unimpeded by scattering would travel from the center to the surface in about 4 fs. This will make surface properties, already crucial for the mobility of hot carriers in bulk semiconductors[63] and devices,[64] even more important for nanocrystals.

If the pulse is much shorter than the scattering time, one can use $d\Delta E_g/dk$ from the band structure and the full width at half-maximum energy bandwidth of the pulse, ΔE_p, to calculate the wave-vector spread $\Delta k = [1/(d\Delta E_g/dk)]\Delta E_p$ and wavepacket width excited by a coherent pulse (a 20 fs pulse at 600 nm would excite a 25 nm wide wavepacket in bulk PbS). As the pulses are longer than the scattering time, the coherence of scattering becomes relevant, especially because phonon deformations of the lattice are almost stationary during the scattering time. Interpreting a 5 fs scattering time as a lifetime, electronic states would be broadened to a full width at half-maximum, $\Delta E = h/(\pi\tau)$, of ~0.25 eV. Such broadening blurs the distinction between bulk and nanocrystals, allows access to a wider range of k than indicated by the pulse spectrum and band structure, and limits the coherence length of optically excited wavepackets (to less than 6 nm for a 5 fs lifetime). In the spatial domain, quantized cyclotron resonances in semiconductors require a total scattering length greater than the retracing path length divided by 2π.[19] For the minimum retracing path (twice the nanocrystal diameter for a 1S state), this is ~2.5 nm for an 8 nm nanocrystal, thus it seems plausible that hot electrons and holes do not support quantum confined electronic states at room temperature.

The above scenario indicates that the high-energy electronic eigenstates of nanocrystals are, like the high-energy bulk band structure, a concept useful only as a basis set. This picture appears to support arguments in favor of a bulklike or surface-mediated impact ionization mechanism in nanocrystals.[7,65] However, if the states generated immediately after impact ionization are quantum confined, then the impact ionization coupling between bulklike and quantum-confined states will be important for the yield. This coupling may be most naturally treated in a quantum-confined basis. Such confinement effects at twice the nanocrystal band gap are necessarily important near the minimum energetic threshold. Qualitatively different results have been reported for the effect of quantum confinement on the density of biexciton states,[35,65] and not all are coupled.[27] Far above threshold, it is not clear what fraction of the states generated immediately after impact ionization (and before subsequent cooling) have a quantum confined character. However, surface-mediated processes, important for hot carriers in the bulk measurements,[63] are likely more important in nanocrystals than in the bulk.

The above scenario justifies a bulklike picture that explains not only the small pump−probe signal, but also the initial negative signal from the smooth background. For bulk semiconductors, absent scattering, the pump−probe signal involves a delicate cancellation between positive and negative signals. Both elastic and inelastic collisions of carriers with phonons will rapidly (within ~5 fs) scatter the hot electrons and holes into different momentum states during the pulse so that Pauli blocking prevents direct emission. The net result is that negative signal from excited state absorption overbalances the positive signal from ground state depopulation. The elastic scattering of carriers by phonons

© 2010 American Chemical Society

DOI: 10.1021/nl1010349 | Nano Lett. 2010, 10, 2498--2505

might underlie the 7 fs electronic dephasing reported in calculations on smaller lead salt quantum dots.[66]

The quantum confined E1 state decays with a lifetime of ~100 fs; this is analogous to intervalley scattering in the bulk[67] and internal conversion in molecules,[68] both of which normally occur on a ~100 fs time scale. This intervalley scattering populates hot bulklike states that relax similarly to those excited directly via the underlying smooth absorption background. The relaxation of these bulklike states can be fit to a 240 fs exponential decay, which is at the slow end of compatibility with the energy relaxation times reported for probing at the band gap[6] and is in reasonable agreement with calculations for electronic energy relaxation in smaller PbSe nanocrystals.[54] While the degenerate pump−probe experiments reported here may not probe the band gap states directly, they should be directly sensitive to the Stark shift of the spectrum that occurs through carrier migration to the nanocrystal surface;[51] this time scale may differ from that of electronic energy relaxation to the band gap.

In conclusion, we have time-resolved intervalley scattering and the development of the Stark shift in semiconductor nanocrystals. Direct measurements of hot electronic dynamics in PbS nanocrystals with 25 fs time resolution suggest that hot electronic excitations are bulklike, uncoupled, and insensitive to the surface properties that affect slower dynamics (such as Auger recombination of multiexciton states produced by either single or multiphoton excitation). Production of multiexciton states has been reported in PbS, PbSe, PbTe, InAs, CdSe, and Si quantum dots.[32] In all five direct gap semiconductors, the bulk band structures predict diverging effective masses and optically excited carrier group velocities exceeding the saturation velocity below the reported threshold for single photon production of biexciton states. Except for electrons in InAs, the mobilities indicate Ohm's law scattering lengths no more than 4× longer than that of PbS. For carriers above the impact ionization threshold in these systems, quantum confinement should not be expected for three reasons: the Bohr exciton radius tends to zero, the carriers are coupled to polarons whose radius tends to zero, and rapid phonon scattering prevents carriers from retracing their orbits without collisions. The scattering length depends on carrier-phonon coupling not considered in the exciton Bohr radius criterion for distinguishing a quantum dot from a small piece of bulk semiconductor. This suggests bulklike scattering dynamics is important for hot carriers in many nanocrystals conventionally regarded as quantum dots.

Acknowledgment. We thank Arthur Nozik for useful discussions. This work was funded by the Division of Chemical Sciences, Geosciences, and Biosciences, Office of Basic Energy Sciences of the U.S. Department of Energy through Grant DE-FG02-07ER15912.

Note Added after ASAP Publication. This paper published ASAP June 15, 2010 with an error in the caption of Figure 4; the correct version published on June 18, 2010.

REFERENCES AND NOTES

(1) Nozik, A. J. *Physica E* **2002**, *14*, 115.
(2) Green, M. A. *Physica E* **2002**, *14*, 65.
(3) Konstantatos, G.; Howard, I.; Fischer, A.; Hoogland, S.; Clifford, J.; Klem, E.; Levina, L.; Sargent, E. H. *Nature* **2006**, *442*, 180.
(4) Klimov, V. I.; Mikhailovsky, A. A.; McBranch, D. W.; Leatherdale, C. A.; Bawendi, M. G. *Science* **2000**, *287*, 1011.
(5) Schaller, R. D.; Agranovich, V. M.; Klimov, V. I. *Nat. Phys.* **2005**, *1*, 189.
(6) Ellingson, R. J.; Beard, M. C.; Johnson, J. C.; Yu, P.; Micic, O. I.; Nozik, A. J.; Shabaev, A.; Efros, A. L. *Nano Lett.* **2005**, *5*, 865.
(7) Franceschetti, A.; An, J. M.; Zunger, A. *Nano Lett.* **2006**, *6*, 2191.
(8) Schaller, R. D.; Klimov, V. I. *Phys. Rev. Lett.* **2004**, *92*, 186601.
(9) Nozik, A. J. *Annu. Rev. Phys. Chem.* **2001**, *52*, 193.
(10) Klingshirn, C. F. *Semiconductor Optics*, Springer Study ed., Corrected Printing; Springer: Berlin, 1997.
(11) Yu, P. Y.; Cardona, M. *Fundamentals of Semiconductors*, 3rd ed.; Springer: New York, 2005.
(12) Shockley, W. *Bell System Tech. J.* **1951**, *30*, 990.
(13) Éfros, A. L.; Éfros, A. L. *Sov. Phys. Semicond.* **1982**, *16*, 772.
(14) Chepic, D. I.; Éfros, A. L.; Ekimov, A. I.; Ivanov, M. G.; Kharchenko, V. A.; Kudriavtsev, I. A.; Yazeva, T. V. *J. Lumin.* **1990**, *47*, 113.
(15) Brus, L. E. *J. Chem. Phys.* **1984**, *80*, 4403.
(16) Yu, P.; Beard, M. C.; Ellingson, R. J.; Ferrere, S.; Curtis, C.; Drexler, J.; Luiszer, F.; Nozik, A. J. *J. Phys. Chem. B* **2005**, *109*, 7084.
(17) Leatherdale, C. A.; Woo, W. K.; Mikulec, F. V.; Bawendi, M. G. *J. Phys. Chem. B* **2002**, *106*, 7619.
(18) Klimov, V. I. *J. Phys. Chem. B* **2000**, *104*, 6112.
(19) Kittel, C. *Introduction to Solid State Physics*, 8th ed.; John Wiley & Sons: New York, 2004.
(20) Brus, L. E. *J. Chem. Phys.* **1983**, *79*, 5566.
(21) Schmitt-Rink, S.; Miller, D. A. B.; Chemla, D. S. *Phys. Rev. B* **1987**, *35*, 8113.
(22) Hanamura, E. *Phys. Rev. B* **1988**, *37*, 1273.
(23) Gaponenko, S. V. *Optical Properties of Semiconductor Nanocrystals*; Cambridge University Press: New York, 1998.
(24) Butcher, P. N.; Cotter, D. *The elements of nonlinear optics*; Cambridge University Press: New York, 1991.
(25) Mukamel, S. *Principles of Nonlinear Optical Spectroscopy*; Oxford University Press: New York, 1995; Vol. 6.
(26) Jonas, D. M.; Fleming, G. R. Vibrationally Abrupt Pulses in Pump-Probe Spectroscopy. In *Ultrafast Processes in Chemistry and Photobiology*; El-Sayed, M. A., Tanaka, I., Molin, Y., Eds.; Blackwell Scientific: Oxford, 1995; p 225.
(27) Rabani, E.; Baer, R. *Nano Lett.* **2008**, *8*, 4488.
(28) Allan, G.; Delerue, C. *Phys. Rev. B* **2006**, *73*, 205423.
(29) Shabaev, A.; Efros, A. L.; Nozik, A. J. *Nano Lett.* **2006**, *6*, 2856.
(30) Ben-Lulu, M.; Mocatta, D.; Bonn, M.; Banin, U.; Ruhman, S. *Nano Lett.* **2008**, *8*, 1207.
(31) Nair, G.; Geyer, S. M.; Chang, L. Y.; Bawendi, M. G. *Phys. Rev. B* **2008**, *78*, 10.
(32) Nozik, A. J. *Chem. Phys. Lett.* **2008**, *457*, 3.
(33) Trinh, M. T.; Houtepen, A. J.; Schins, J. M.; Hanrath, T.; Piris, J.; Knulst, W.; Goossens, A.; Siebbeles, L. D. A. *Nano Lett.* **2008**, *8*, 1713.
(34) McGuire, J. A.; Joo, J.; Pietryga, J. M.; Schaller, R. D.; Klimov, V. I. *Acc. Chem. Res.* **2008**, *41*, 1810.
(35) Pijpers, J. J. H.; Ulbricht, R.; Tielrooij, K. J.; Osherov, A.; Golan, Y.; Delerue, C.; Allan, G.; Bonn, M. *Nat. Phys.* **2009**, *5*, 811.
(36) Ji, M. B.; Park, S.; Connor, S. T.; Mokari, T.; Cui, Y.; Gaffney, K. J. *Nano Lett.* **2009**, *9*, 1217.
(37) Ravich, Y. I. Lead Chalcogenides: Basic Physical Features. In *Lead Chalcogenides: Physics & Applications*; Khokhlov, D., Ed.; Taylor and Francis: New York, 2003; p 3.
(38) Wise, F. W. *Acc. Chem. Res.* **2000**, *33*, 773.
(39) Jha, P. P.; Guyot-Sionnest, P. *ACS Nano* **2009**, *3*, 1011.
(40) Siegman, A. E. *Lasers*; University Science Books: Mill Valley, CA, 1986.
(41) Cademartiri, L.; Montanari, E.; Calestani, G.; Migliori, A.; Guagliardi, A.; Ozin, G. A. *J. Am. Chem. Soc.* **2006**, *128*, 10337.

© 2010 American Chemical Society

DOI: 10.1021/nl1010349 | *Nano Lett.* **2010,** *10,* 2498--2505

(42) Moreels, I.; Lambert, K.; De Muynck, D.; Vanhaecke, F.; Poelman, D.; Martins, J. C.; Allan, G.; Hens, Z. *Chem. Mater.* **2007**, *19*, 6101.
(43) Kanazawa, H.; Adachi, S. *J. Appl. Phys.* **1998**, *83*, 5997.
(44) Kohn, S. E.; Yu, P. Y.; Petroff, Y.; Shen, Y. R.; Tsang, Y.; Cohen, M. L. *Phys. Rev. B* **1973**, *8*, 1477.
(45) Koole, R.; Allan, G.; Delerue, C.; Meijerink, A.; Vanmaekelbergh, D.; Houtepen, A. J. *Small* **2008**, *4*, 127.
(46) Brus, L. *IEEE J. Quantum Electron.* **1986**, *QE-22*, 1909.
(47) Piel, J.; Riedle, E.; Gundlach, L.; Ernstorfer, R.; Eichberger, R. *Opt. Lett.* **2006**, *31*, 1289.
(48) Paye, J. *IEEE J. Quantum Electron.* **1994**, *30*, 2693.
(49) Hyun, B.-R.; Zhong, Y.-W.; Bartnik, A. C.; Sun, L.; Abruña, H. D.; Wise, F. D.; Goodreau, J. D.; Matthews, J. R.; Leslie, T. M.; Borrelli, N. F. *ACS Nano* **2008**, *2*, 2206.
(50) Peterson, J. J.; Krauss, T. D. *Nano Lett.* **2006**, *6*, 510.
(51) Norris, D. J.; Sacra, A.; Murray, C. B.; Bawendi, M. G. *Phys. Rev. Lett.* **1994**, *72*, 2612.
(52) Cardona, M.; Greenaway, D. L. *Phys. Rev. A* **1964**, *133*, 1685.
(53) Brus, L. *Appl. Phys. A* **1991**, *53*, 465.
(54) Kilina, S. V.; Craig, C. F.; Kilin, D. S.; Prezhdo, O. V. *J. Phys. Chem. C* **2007**, *111*, 4871.
(55) Stouwdam, J. W.; Shan, J.; van Veggel, F.; Pattantyus-Abraham, A. G.; Young, J. F.; Raudsepp, M. *J. Phys. Chem. C* **2007**, *111*, 1086.
(56) Klimov, V. I.; McGuire, J. A.; Schaller, R. D.; Rupasov, V. I. *Phys. Rev. B* **2008**, *77*, 195324.
(57) Sykora, M.; Koposov, A. Y.; McGuire, J. A.; Schulze, R. K.; Tretiak, O.; Pietryga, J. M.; Klimov, V. I. *ACS Nano* **2010**, *4*, 2021.
(58) Romero, A. H.; Cardona, M.; Kremer, R. K.; Lauck, R.; Siegle, G.; Serrano, J.; Gonze, X. C. *Phys. Rev. B* **2008**, *78*, 224302.
(59) Ryder, E. J. *Phys. Rev.* **1953**, *90*, 766.
(60) Shockley, W. *Electrons and Holes in Semiconductors with Applications to Transistor Electronics*; D. Van Nostrand Company, Inc: Princeton, NJ, 1966.
(61) Sze, S. M. *Physics of Semiconductor Devices*; Wiley-Interscience: New York, 1969.
(62) Higman, J. M.; Hess, K.; Hwang, C. G.; Dutton, R. W. *IEEE Trans. Electron Devices* **1989**, *36*, 930.
(63) Ryder, E. J.; Shockley, W. *Phys. Rev.* **1951**, *81*, 139.
(64) Fischetti, M. V.; Laux, S. E.; Crabbe, E. *J. Appl. Phys.* **1995**, *78*, 1058.
(65) Luo, J.-W.; Franceschetti, A.; Zunger, A. *Nano Lett.* **2008**, *8*, 3174.
(66) Kamisaka, H.; Kilina, S. V.; Yamashita, K.; Prezhdo, O. V. *Nano Lett.* **2006**, *6*, 2295.
(67) Shank, C. V.; Becker, P. Femtosecond Processes in Semiconductors. In *Spectroscopy of Nonequilibrium Electrons and Phonons*; Shank, C. V., Zakharchenya, B. P., Eds.; Elsevier: Amsterdam, 1992; p 215.
(68) Fleming, G. R. *Chemical Applications of Ultrafast Spectroscopy*; Oxford University Press: New York, 1986.

© 2010 American Chemical Society

DOI: 10.1021/nl1010349 | *Nano Lett.* **2010,** *10,* 2498--2505